Inelastic Scattering in Low-Energy Electron Diffraction from Silver*

WILLES H. WEBER† AND MAURICE B. WEBB
University of Wisconsin, Madison, Wisconsin 53706
(Received 1 July 1968)

In a low-energy electron diffraction experiment on Ag (111) we have studied the inelastically scattered current of electrons having lost $\lesssim 10$ eV. We show quantitatively that this current, which is strongly peaked in the directions of Bragg reflections, arises from a two-step process involving both an elastic and an inelastic scattering. A model based on the two-step process is developed and then compared with experimental results. The model allows one to separate the Bragg and phonon components of the inelastic scattering and to extract an energy-loss spectrum which is independent of the elastic scattering. The structure, intensity, angular widths, and angle-of-incidence dependence of the energy-loss spectra are compared with the predictions of a dielectric-constant energy-loss formalism using known optical constants. The comparison, which includes both surface and volume losses, shows reasonable agreement and indicates that the surface losses predominate.

I. INTRODUCTION

IN 1938 Turnbull and Farnsworth[1] investigated the inelastic scattering of low-energy electrons from silver using a magnetic analyzer and observed peaks in the energy-loss spectrum at 3.9 and 7.3 eV. These electrons were concentrated about the directions of the elastically scattered beams. The authors suggested that this observation is consistent with an earlier suggestion of Davisson and Germer[2] that the inelastic electrons result from a two-step process consisting of a Bragg reflection and an energy loss. When incident electrons with energy the order of 100 eV interact with the loosely bound electrons and lose a small fraction of their energy, the momentum transfer is small. Their subsequent Bragg reflection then results in inelastic beams near the elastic ones.

More recently Tharp and Scheibner,[3] using a hemispherical collector and a retarding potential, have measured the energy distribution of the electrons inelastically scattered from the (110) surface of tungsten. They attributed peaks in the energy-loss spectrum to surface and bulk plasma losses and to interband transitions. The intensity in the plasma-loss peak changed with adsorption of oxygen in the same way as the elastic current, again suggesting the two-step process.

Characteristic energy losses in Ag were first studied by Rudberg[4] in reflection experiments from amorphous layers deposited under vacuum. In additional experiments on Ag using transmission[5–7] and reflection[1,8] techniques, there has been general agreement on the structure of the energy-loss spectrum, i.e., there is a large narrow peak near $\Delta E=3.7$ eV and a smaller peak near $\Delta E=7.5$ eV. Powell and Swan[9] in reflection experiments on Al demonstrated the importance of surface contamination on energy-loss studies and experimentally verified the existence of the surface plasmons predicted by Ritchie.[10] Surface plasma losses have been studied in several subsequent experiments.[11–13] In recent transmission experiments on very thin films, Raether[14] has been able to resolve the low-lying loss in silver into two peaks: one at $\Delta E=3.6$ eV, which is interpreted as a surface loss, and one at $\Delta E=3.78$ eV, which is interpreted as a volume loss.

The theoretical description of characteristic energy losses which has been most successful in explaining experimental results is the phenomenological dielectric constant formalism. The theory is due to Fermi,[15] Hubbard,[16] Frölich,[17] and Frölich and Pelzer,[18] and it has been reviewed by Raether.[19] The energy lost by an energetic incident electron is calculated self-consistently by considering the absorption of energy from the Fourier components of its electric field by a medium whose response can be described by a complex, frequency- and wave-vector-dependent dielectric constant $\epsilon(\mathbf{q},\omega)$. In an infinite medium the calculation leads to a differential probability per unit path length that the electron loses energy ΔE and is scattered through an angle θ. These losses, which are called bulk losses, are peaked at $\mathrm{Re}(\epsilon)=0$. Several authors[10,20–22] have shown that the

* Work supported by the U. S. Air Force Office of Scientific Research under Grant No. AF-AFOSR-51-66.

† Present address: Scientific Laboratory, Ford Motor Co., Dearborn, Mich.

[1] J. C. Turnbull and H. E. Farnsworth, Phys. Rev. **54**, 509 (1938).
[2] C. J. Davisson and L. H. Germer, Phys. Rev. **30**, 705 (1927).
[3] L. N. Tharp and E. J. Scheibner, J. Appl. Phys. **38**, 3320 (1967). See also E. J. Scheibner and L. N. Tharp, Surface Sci. **8**, 247 (1967).
[4] R. Rudberg and J. C. Slater, Phys. Rev. **50**, 138 (1936).
[5] C. Kunz, Z. Physik **167**, 53 (1962).
[6] A. Otto and W. Steinmann, Phys. Status Solidi **2**, K187 (1962).
[7] W. Steinmann, Phys. Rev. Letters **5**, 470 (1960).
[8] J. L. Robins, Proc. Phys. Soc. (London) **78**, 1177 (1961).
[9] C. J. Powell and J. B. Swan, Phys. Rev. **115**, 869 (1959).
[10] R. H. Ritchie, Phys. Rev. **106**, 874 (1957).
[11] P. Schmueser, Z. Physik **180**, 105 (1964).
[12] A. Otto, Z. Physik **185**, 232 (1965).
[13] L. K. Jordan and E. F. Scheibner, Surface Sci. **10**, 373 (1968).
[14] H. Raether, Surface Sci. **8**, 233 (1967).
[15] E. Fermi, Phys. Rev. **57**, 485 (1940).
[16] J. Hubbard, Proc. Phys. Soc. (London) **A68**, 976 (1955).
[17] H. Frölich, *Max-Planck-Festschrift* (VEB Deutscher Verlag der Wissenschaften, Berlin, 1958), p. 277.
[18] H. Frölich and H. Pelzer, Proc. Phys. Soc. (London) **A68**, 525 (1955).
[19] H. Raether, Ergeb. Exakt. Naturw. **38**, 84 (1965).
[20] N. Takimoto, Phys. Rev. **146**, 366 (1966).
[21] A. Otto, Phys. Status Solidi **22**, 401 (1967).
[22] P. A. Fedders, Phys. Rev. **153**, 438 (1967).

boundary conditions at the surface lead to additional losses, called surface losses, which are peaked at $\mathrm{Re}(\epsilon)=-1$, if the medium is bounded by vacuum. The differential probabilities for both surface and bulk losses are strongly peaked in the forward direction with a half-width of magnitude $(\Delta E/E_0)$. There is general agreement between this theoretical description and experimental results observed in transmission experiments.[19,23,24]

It is the primary purpose of this work to establish quantitatively the two step process in the inelastic scattering of low-energy electrons and to extract an energy-loss spectrum and angular spreading, independent of the elastic scattering, which can be compared with theoretical calculations. The apparatus and pertinent experimental details are described briefly in Sec. II. An expression for the observed inelastic intensity from the two-step process is derived in Sec. III. The experimental results are presented in Sec. IV, and these are compared with the phenomenological dielectric-constant formalism using known optical constants in Sec. V. This comparison shows that the surface losses predominate in these experiments.

II. EXPERIMENTAL

The essential parts of the apparatus have been described before.[25] These include an electron gun, a goniometer, a Faraday collector, and nested planar grids and fluorescent screen all contained in a stainless-steel ultrahigh vacuum system.

The electron gun has a tungsten filament operating at 2500°K and provides a beam of a few tenths of a microampere. The beam has a diameter of ≈ 0.3 mm at the crystal and a divergence of $<0.5°$.

The crystal is mounted in the two-circle goniometer with an azimuthal axis normal to the crystal surface and a tilt axis in the plane of the surface. Angles can be measured absolutely to 0.5° and changes in the angles can be measured to 0.025°. The goemetry of the experiments in reciprocal space and the notation for the pertinent angles are shown in Fig. 1.

The Faraday collector is mounted on a yoke which rotates about an axis collinear with the tilt axis of the goniometer. The detector consists of an outer can, at the potential of the crystal, surrounding an inner cup which is the actual collector and whose potential can be varied to analyze the energy of the scattered electrons. A circular aperture in the outer can has an angular diameter of 2.6° at the crystal. Guard electrodes eliminate leakage currents from the measurements.

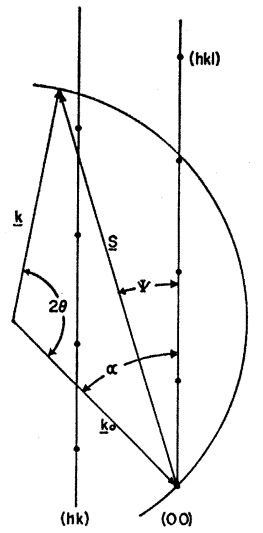

FIG. 1. Reciprocal lattice for weakly penetrating radiation showing the Ewald construction and defining the notation used in the text. 2θ is the scattering angle, α is the angle of incidence, and Ψ is the angle between S and the (00) rod.

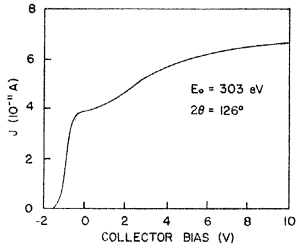

(a)

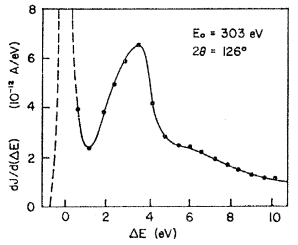

(b)

FIG. 2. (a) Recorder tracing of the measured current as a function of the collector voltage. (b) Energy-loss spectrum.

The energy of the scattered electrons was analyzed by varying the potential of the inner cup from a few volts below to 10 or 20 V above the potential of the gun filament. The measured current was recorded as a function of this retarding potential giving an integrated energy spectrum, an example of which is shown in Fig. 2(a). Differentiating gives the energy spectrum, i.e., $dJ/d(\Delta E)$ as a function of ΔE. The energy loss ΔE is measured from the elastic peak. An example of an energy-loss spectrum is shown in Fig. 2(b). The energy resolution is given by the full width at half-maximum of the elastic peak and is about 0.5 eV. This width comes from two sources, the thermal spread of the incident beam and the geometry of the retarding fields in the finite aperture.

The experiments were done on a (111) face of a silver crystal, prepared as described in Ref. 25.

[23] M. Creuzberg and H. Raether, Solid State Commun. **2**, 175 (1964).
[24] N. Swanson, Phys. Rev. **165**, 1067 (1968).
[25] E. R. Jones, J. T. McKinney, and M. B. Webb, Phys. Rev. **151**, 476 (1966).

III. MODEL DERIVATION

In this section we derive an expression for the inelastic intensity from the two-step process. We assume that only single-energy losses are important and that the elastic and inelastic scatterings are independent.[26]

First we treat only the surface losses and assume these take place either at or outside the crystal surface. Consider an incident beam of unit intensity, energy E_0, and propagation vector $\mathbf{k}_0$. Let $d^2p(\Delta E, \mathbf{k}_0 \rightarrow \mathbf{k}')/d(\Delta E)d\Omega$ be the probability per unit solid angle and energy loss that an electron loses energy ΔE and is scattered into the direction of $\mathbf{k}'$. This then gives the beam of inelastic electrons incident on the crystal which subsequently are elastically scattered. Let $I_{\text{elastic}}(E_0-\Delta E, \mathbf{k}' \rightarrow \mathbf{k})$ be the probability per unit solid angle that an electron of energy $E_0-\Delta E$ and propagation vector $\mathbf{k}'$ is elastically scattered into the direction of $\mathbf{k}$. Then the contribution to the inelastic intensity per unit solid angle in the direction of $\mathbf{k}$ from those electrons which first lose energy and then are elastically scattered is found by integrating over intermediate states,

$$\frac{dI(\Delta E,k)}{d(\Delta E)}=\int \frac{d^2p(\Delta E, \mathbf{k}_0 \rightarrow \mathbf{k}')}{d(\Delta E)d\Omega} \times I_{\text{elastic}}(E_0-\Delta E, \mathbf{k}' \rightarrow \mathbf{k})d\Omega_{\mathbf{k}'}. \quad (1)$$

If we now restrict the elastic scattering to include only Bragg reflections, the Ewald construction selects only those directions $\mathbf{k}'$ such that $\mathbf{k}'+\mathbf{G}_i=\mathbf{k}$, where $\mathbf{G}_i$ is a reciprocal-lattice vector. Letting $J_{i,\text{Bragg}}$ be the measured Bragg reflected current for unit incident current in direction $\mathbf{k}'$, integrating Eq. (1) gives

$$\left(\frac{dI(\Delta E,\mathbf{k})}{d(\Delta E)}\right)_{\text{Bragg}}=\sum_{\mathbf{G}_i} \frac{d^2p(\Delta E, \mathbf{k}_0 \rightarrow \mathbf{k}-\mathbf{G}_i)}{d(\Delta E)d\Omega} \times J_{i,\text{Bragg}}(E_0-\Delta E, \mathbf{k}-\mathbf{G}_i). \quad (2)$$

The contribution to the measured inelastic current $[dJ/d(\Delta E)]'_{\text{Bragg}}$ is Eq. (2) integrated over the detector:

$$\left(\frac{dJ}{d(\Delta E)}\right)'_{\text{Bragg}}=\int_{\Omega_D} \frac{d^2p(\Delta E, \mathbf{k}_0 \rightarrow \mathbf{k}-\mathbf{G})}{d(\Delta E)d\Omega} \times J_{\text{Bragg}}(E_0-\Delta E, \mathbf{k}-\mathbf{G})d\Omega_{\mathbf{k}},$$

where only one term contributes to the integral since $d^2p/d(\Delta E)d\Omega$ is strongly peaked in the forward direction. For the detector centered on a (00) reflection, assuming J_{Bragg} is a slow function of the angle of incidence, it can be replaced by its value at the center of the region of integration and taken outside the integral giving

$$\left(\frac{dJ}{d(\Delta E)}\right)'_{\text{Bragg}}=\int_{\Omega_D} \frac{d^2p(\Delta E, \mathbf{k}_0 \rightarrow \mathbf{k}-\mathbf{G})}{d(\Delta E)d\Omega}d\Omega_{\mathbf{k}} \times J_{\text{Bragg}}(E_0-\Delta E). \quad (3)$$

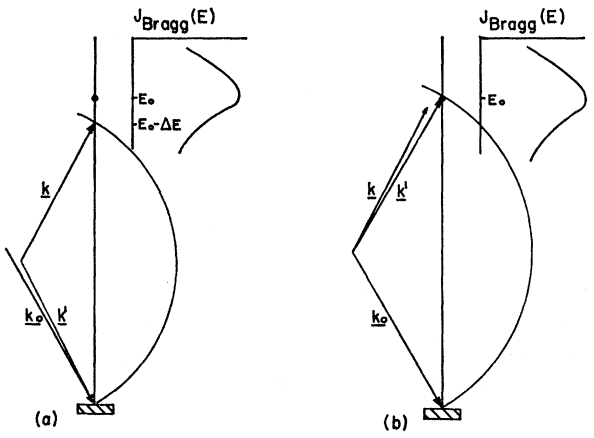

FIG. 3. Schematic drawing showing the contributions to the inelastic current in the direction of $\mathbf{k}$ for a (00) reflection in which the energy loss occurs (a) before and (b) after the Bragg reflection.

The geometry for a single value of $\mathbf{k}$ is illustrated in Fig. 3(a).

There is an additional contribution, illustrated in Fig. 3(b), from electrons which are first Bragg reflected and then elastically scattered. This is calculated in the same way as above and differs mainly in that the Bragg reflection occurs at E_0 instead of at $E_0-\Delta E$.

If $d^2p/d(\Delta E)d\Omega$ is the same for electrons approaching or leaving the crystal at the same angle, the sum of both the surface-loss contributions is

$$\left(\frac{dJ}{d(\Delta E)}\right)_{\text{Bragg}}=\int_{\Omega_D} \frac{d^2p(\Delta E)}{d(\Delta E)d\Omega}d\Omega \times\{J_{\text{Bragg}}(E_0-\Delta E)+J_{\text{Bragg}}(E_0)\}, \quad (4)$$

where the angular arguments have been dropped and the integration is over the solid angle of the detector centered in the forward direction.

We now consider the contribution to the inelastic intensity from electrons which lose energy as they move through the crystal. For these volume losses the inelastic scattering is described by $d^2(1/\Lambda)(\Delta E, \mathbf{k}_0 \rightarrow \mathbf{k}')/d(\Delta E)d\Omega$, the differential probability per unit path length per unit solid angle and energy loss that an electron loses energy ΔE and is scattered into the direction of $\mathbf{k}'$. The calculation is similar to that above except we must account for the attenuation of the beam due to all the inelastic and elastic processes. We assume the beam is attenuated as $\exp(-\mu x)$ where μ is a linear attenuation coefficient independent of direction and a slow function of energy.[25]

[26] This latter assumption is made plausible considering second-order time-dependent perturbation theory with an interaction Hamiltonian with two terms: one giving the elastic Bragg scattering and one an inelastic scattering. The resulting terms involving interference between the two processes are negligible because of their energy denominators.

First we find the contribution from those electrons which lose energy between the nth and $(n+1)$th atomic planes. These make a beam of inelastic electrons incident on the half-crystal bounded by the $(n+1)$th atomic plane whose intensity is given by

$$e^{-\mu nd/\cos\alpha}(d/\cos\alpha) \times[d^2\{1/\Lambda(\Delta E, \mathbf{k}_0 \to \mathbf{k})\}/d(\Delta E)d\Omega]d(\Delta E)d\Omega,$$

where d is the interplanar spacing. Now the problem is just like that for the surface losses and this beam gives a Bragg reflected intensity proportional to $J_{\text{Bragg}}(E_0-\Delta E)$ which is then further attenuated on the way out of the crystal. For the (00) reflection the attenuation factor is $\exp(-\mu nd/\cos\alpha)$, therefore

$$\left(\frac{dJ_{n,n+1}}{d(\Delta E)}\right)'_{\text{Bragg}} = e^{-2\mu nd/\cos\alpha}(d/\cos\alpha) \times\int_{\Omega_D}\frac{d^2(1/\Lambda)}{d(\Delta E)d\Omega}d\Omega J_{\text{Bragg}}(E_0-\Delta E). \quad (5)$$

Adding the contribution from electrons which are Bragg reflected before the inelastic scattering and then summing Eq. (5) over n gives

$$\left(\frac{dJ}{d(\Delta E)}\right)_{\text{Bragg}} = \frac{e^{-2\mu d/\cos\alpha}}{1-e^{-2\mu d/\cos\alpha}}(d/\cos\alpha) \times\int_{\Omega_D}\frac{d^2(1/\Lambda)}{d(\Delta E)d\Omega}d\Omega\{J_{\text{Bragg}}(E_0-\Delta E)+J_{\text{Bragg}}(E_0)\}. \quad (6)$$

The total inelastic intensity associated with the Bragg reflection and including both surface and bulk losses is the sum of Eqs. (4) and (6);

$$\left(\frac{dJ}{d(\Delta E)}\right)_{\text{Bragg}} = \frac{dP}{d(\Delta E)} \times\{J_{\text{Bragg}}(E_0-\Delta E)+J_{\text{Bragg}}(E_0)\}, \quad (7)$$

where

$$\frac{dP}{d(\Delta E)} = \frac{e^{-2\mu d/\cos\alpha}}{1-e^{2\mu d/\cos\alpha}}(d/\cos\alpha)\int_{\Omega_D}\frac{d^2(1/\Lambda)}{d(\Delta E)d\Omega}d\Omega + \int_{\Omega_D}\frac{d^2p}{d(\Delta E)d\Omega}d\Omega.$$

In addition to the Bragg reflections, $I_{\text{elastic}}(E)$ contains diffuse phonon scattering, which is considered elastic in these experiments. This scattering has not been included in Eqs. (2)–(7). The bragg scattering is $\exp(-2M)$ times that from the rigid lattice, where $\exp(-2M)$ is the Debye-Waller factor and $2M$ is proportional to T in the high-temperature Debye approximation. The integrated phonon scattering is proportional to $[1-\exp(-2M)]$.[27] Since $2M$ is large (between 1 and 4 in typical experiments), this phonon scattering is a large part of the elastic current, even though it makes only a relatively small contribution in the directions of the Bragg reflections. Rewriting Eq. (2) for the contribution from the diffuse scattering gives

$$\left(\frac{dI(\Delta E,\mathbf{k})}{d(\Delta E)}\right)_{\text{phonon}} = \int\frac{d^2p(\Delta E, \mathbf{k}_0 \to \mathbf{k}')}{d(\Delta E)d\Omega} \times I_{\text{phonon}}(E_0-\Delta E, \mathbf{k}' \to \mathbf{k})d\Omega_{k'}.$$

Although the one-phonon part of this is peaked on the reciprocal-lattice rods, it is very flat compared to the Bragg scattering, and for our purposes it is sufficient to assume that the phonon scattering is uniform. With this assumption the measured inelastic intensity from surface losses associated with the phonon scattering is [analogous to Eq. (4)]

$$\left(\frac{dJ}{d(\Delta E)}\right)_{\text{phonon}} = \int\frac{d^2p(\Delta E)}{d(\Delta E)d\Omega}d\Omega \times\{J_{\text{phonon}}(E_0-\Delta E)+J_{\text{phonon}}(E_0)\}, \quad (8)$$

where the integral is over all solid angles. One obtains an expression for the total diffuse inelastic intensity which is identical in form to Eq. (7), but which has a different factor $dP/d(\Delta E)$ because of the different limits on the angular integrations.

The assumptions that the surface losses take place outside or at the surface of the crystal and that the probability for bulk losses is independent of depth are perhaps too simple. However, it is clear that these assumptions do not affect the form of Eq. (7), in particular the dependence of the inelastic current on $\{J_{\text{Bragg}}(E_0-\Delta E)+J_{\text{Bragg}}(E_0)\}$.

IV. RESULTS

In this section we present the experimental results and compare them with the predictions of Eq. (7). First, to show that the observed inelastic current is indeed associated with the elastic scattering, and to show the separation of the data into $(dJ/d(\Delta E))_{\text{Bragg}}$ and $(dJ/d(\Delta E))_{\text{phonon}}$, we examine the temperature dependence. In Fig. 4, measured energy-loss spectra are plotted for various temperatures. These data were taken on the (00) reciprocal-lattice rod at $E_0=214$ eV and $2\theta=126°$, corresponding to the (555) Bragg reflection.

Assuming $dP/d(\Delta E)$ is temperature-independent, the temperature dependence of $(dJ/d(\Delta E))_{\text{Bragg}}$ should be that of $\{J_{\text{Bragg}}(E_0-\Delta E)+J_{\text{Bragg}}(E_0)\}$. Since $\Delta E/E_0$ is small, the Debye-Waller factors for each of the elastic terms are essentially the same (for $E_0=214$ and $\Delta E<10$

[27] R. F. Barnes, Ph.D. thesis, University of Wisconsin, 1967 (unpublished). See also R. F. Barnes, M. G. Lagally, and M. B. Webb, Phys. Rev. 171, 627 (1968).

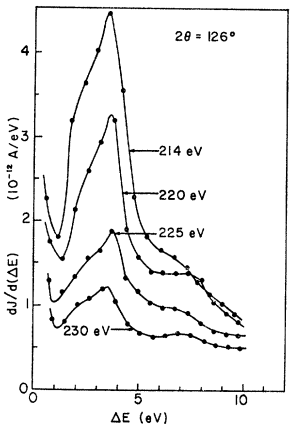

FIG. 4. Energy-loss spectra at various temperatures for the detector centered on a (00) reflection with $E_0=214$ eV and $2\theta=126°$.

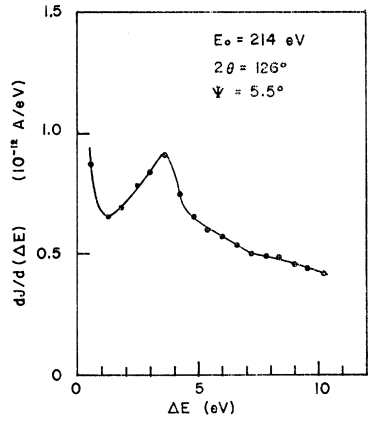

FIG. 6. Phonon contribution to the energy-loss spectrum. These data are for $E_0=214$ eV, $T=24°C$, $2\theta=126°$, and $\Psi=5.5°$ (which corresponds to the zone boundary).

eV they differ by less than 5%), and $(dJ/d(\Delta E))_{\text{Bragg}}$ should be proportional to $\exp(-2M)$.

The temperature dependence of the observed inelastic intensity at $\Delta E=6$ eV is plotted as curve 1 in Fig. 5. The nonlinearity is due to the contribution of $(dJ/d(\Delta E))_{\text{phonon}}$. This phonon contribution can be measured separately at the Brillouin zone boundary and is shown in Fig. 6. This and the elastic phonon scattering[26] at the zone boundary are both essentially temperature-independent in the range of these experiments. We now subtract this phonon contribution and replot $\{dJ/d(\Delta E)-(dJ/d(\Delta E))_{\text{phonon}}\}$ versus T as curve 2 in Fig. 5. This plot is linear and gives the same Debye-Waller factor measured for the elastic scattering. For comparison the temperature dependence of the Bragg scattering plotted in arbitrary units is shown as curve 3 in Fig. 5. Similar agreement is obtained using this procedure for each of several values of ΔE. This result then establishes the connection between the elastic and inelastic scattering and gives a procedure to extract $(dJ/d(\Delta E))_{\text{Bragg}}$.

We now demonstrate that the inelastic scattering is proportional to the particular combination of the elastic currents given in Eq. (7). This is done by measuring energy-loss spectra for several incident energies in the vicinity of a third-Laue-condition peak on the (00) reciprocal-lattice rod. In Fig. 7, we plot the elastic intensity on the (00) reciprocal-lattice rod as a function of energy. It shows that the relative magnitudes of $J_{\text{Bragg}}(E_0-\Delta E)$ and $J_{\text{Bragg}}(E_0)$ change rapidly when the incident energy is changed only a few percent, and thus the energy-loss spectrum will also change rapidly with E_0. However, if the variation in $dP/d(\Delta E)$ in this range of energies is small, the quantity

$$\left(\frac{dJ}{d(\Delta E)}\right)_{\text{Bragg}}/\{J_{\text{Bragg}}(E_0-\Delta E)+J_{\text{Bragg}}(E_0)\}$$

should be independent of E_0.

In Fig. 8 we show the energy-loss spectra measured at various incident energies in the vicinity of the (555) peak. The diffuse contributions determined at the zone boundary are subtracted from these data and then the curves are divided by measured values of $\{J_{\text{Bragg}}(E_0-\Delta E)+J_{\text{Bragg}}(E_0)\}$. The results are plotted in Fig. 9. The fact that these energy-loss spectra coalesce verifies the particular dependence on the elastic current.

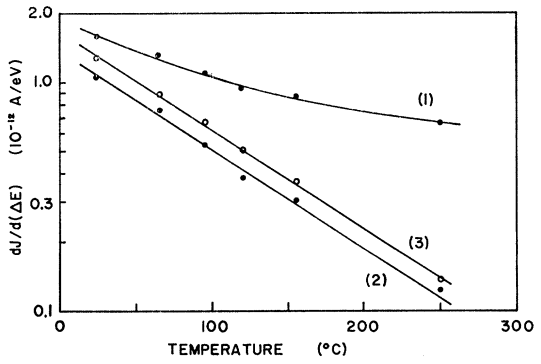

FIG. 5. Curve 1 is the temperature dependence of the inelastic intensity at $\Delta E=6$ eV from Fig. 4. Curve 2 is $(dJ/d(\Delta E))_{\text{Bragg}}$ determined by subtracting the phonon contribution from curve 1. Curve 3 is a plot of the elastic Bragg scattering in arbitrary units showing the same temperature dependence as $(dJ/d(\Delta E))_{\text{Bragg}}$.

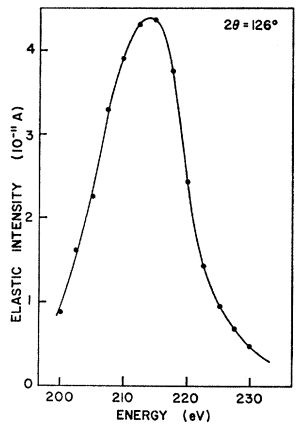

FIG. 7. Measured elastic current versus the incident energy on the (00) reciprocal-lattice rod showing the (555) peak. $T=24°C$ and $2\theta=126°$.

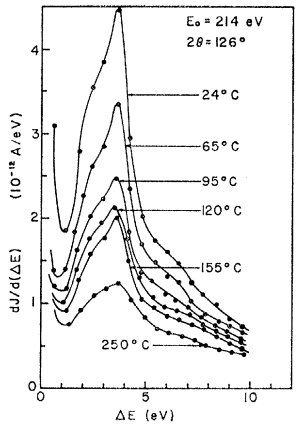

FIG. 8. Energy-loss spectra at various incident energies for the same experimental situation as in Fig. 7.

Thus, the inelastic scattering contains the expected contributions from electrons which are elastically reflected both before and after an inelastic process, and the probabilities for inelastic processes are the same entering and leaving the crystal. Figure 9 shows the factor $dP/d(\Delta E)$ of Eq. (7), which will be compared to theoretical calculations in Sec. V.

The assumption that multiple inelastic scatterings are unimportant for small ΔE may be now checked. The double inelastic scattering is given by the energy and angular convolution of the single scattering. An overestimate of this quantity is given by the energy convolution of $dP/d(\Delta E)$ with itself. Evaluating this for the data shown in Fig. 9 gives an upper limit to the double-loss contributions of 8% at $\Delta E=5$ eV and 30% at $\Delta E=10$ eV. Therefore, to insure that single losses are the major part of the energy-loss spectrum, we must restrict ΔE to values less than 10 eV.

We next present measurements of the angular spreading due to the inelastic scattering. For a fixed incident energy, energy-loss spectra were measured at each of several values of Ψ near the (00) reciprocal-lattice rod; the values of $(dJ/d(\Delta E))_{\text{Bragg}}$ for a given ΔE were then plotted versus Ψ. Two examples are shown in Fig. 10. These data are for $E_0=101$ eV, at which incident energy

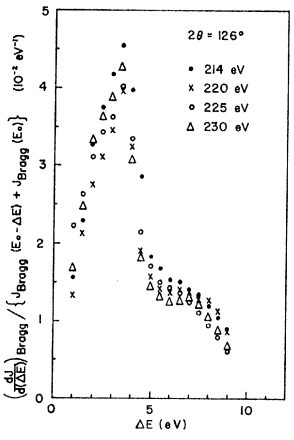

FIG. 9. Shows that the energy-loss spectra in Fig. 8, after being corrected for the phonon scattering and divided by the appropriate Bragg currents, all yield the same quantity $dP/d(\Delta E)$, defined in Eq. (7).

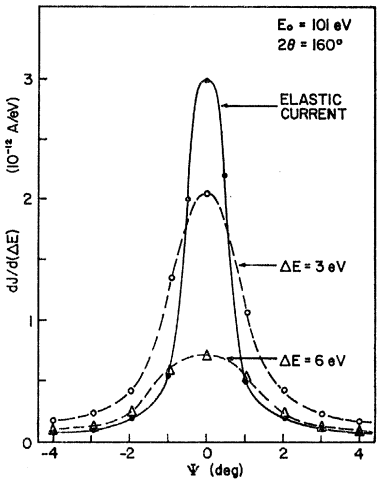

FIG. 10. Inelastic intensity versus Ψ showing the additional angular spreading due to the inelastic scattering. The solid curve is the elastic current plotted in arbitrary units. $E_0=101$ eV and $2\theta=160°$.

the tip of S crossed the rod at the postion of the (444) reflection.

In the present experiments it was necessary to use a relatively large aperture so we need to account for the instrumental width. The elastic scattering as a function of Ψ is also shown in Fig. 10. Since previous higher-resolution experiments[28] show that this is broad compared to the physical width of the reflection, this elastic scattering gives a good approximation to the instrumental function with the present detector. The difference in full widths at half-maximum of the elastic and inelastic peaks is then a measure of the angular spreading in the inelastic scattering.

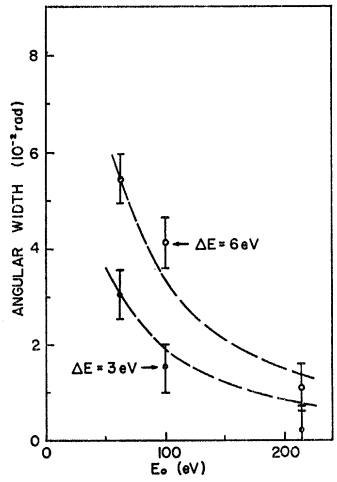

FIG. 11. Angular widths of inelastic peaks versus the incident energy determined by the difference between the measured full widths of $dJ/d(\Delta E)_{\text{Bragg}}$ and J_{Bragg}.

[28] J. T. McKinney, E. R. Jones, and M. B. Webb, Phys. Rev. **160**, 523 (1967). See, also, Refs. 25 and 26.

Angular widths of the inelastic beams determined in this way are plotted against the incident energy in Fig. 11. The dashed lines are plots of $\Delta E/E_0$ normalized at 60 eV and indicate the inelastic widths are roughly proportional to this quantity as expected. The relatively poor resolution of the present experiments precludes measurement of the angular profile of the inelastic scattering.

Finally, we present a determination of the angle-of-incidence dependence of the inelastic scattering. This dependence will be indicative of the relative importance of the surface and bulk losses, since these depend quite differently on the angle of incidence. The experiment was done for specular reflection at a high temperature, where the measured inelastic current is entirely $(dJ/d(\Delta E))_{\text{phonon}}$; in fact, at the energy and temperature of this experiment, $E_0=240$ eV and $T=430°$C, the zero-phonon elastic scattering was not detectable. The factor $dP/d(\Delta E)$ for the phonon scattering should have the same angle-of-incidence dependence as the factor for the Bragg scattering and the high-temperature experiment has the advantage that no separation of these components is necessary.

An example of the results is shown in Fig. 12, where

$$(dJ/d(\Delta E))_{\text{phonon}}/\{J_{\text{phonon}}(E_0-\Delta E)+J_{\text{phonon}}(E_0)\}$$

at $\Delta E=3.8$ eV (corresponding to the prominent low-lying loss) is plotted versus the angle of incidence α. The solid curve is a plot of the angle-of-incidence dependence of the bulk-loss term from Eq. (6) with $\mu=0.2$ Å^{-1}; the dashed curve is a plot of $1/\cos\alpha$, which is approximately the dependence expected for the surface losses, as will be discussed in Sec. V.

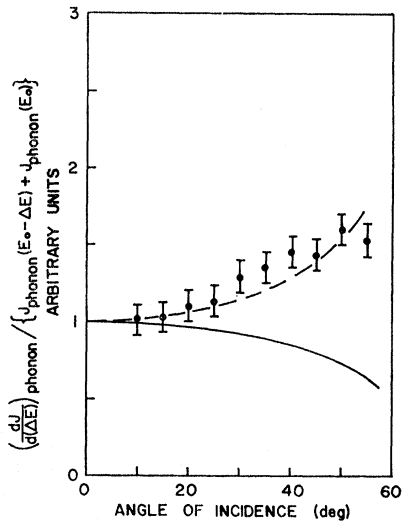

FIG. 12. Angle-of-incidence dependence of the quantity $[dJ/d(\Delta E)]_{\text{phonon}}/[J_{\text{phonon}}(E_0-\Delta E)+J_{\text{phonon}}(E_0)]$. At each value of α the detector is set at the position corresponding to specular reflection. $\Delta E=3.8$ eV, $T=430°$C, and $E_0=240$ eV.

V. COMPARISON TO THEORY AND DISCUSSION

In this section we present a comparison between the experimental energy-loss spectra and the phenomenological dielectric-constant formalism. In an infinite medium the theory gives the following expression for the differential probability per unit path length for the electron to lose energy ΔE and be scattered through the angle θ:

$$\frac{d^2(1/\Lambda)}{d(\Delta E)d\Omega}=\frac{1}{2\pi^2 a_0 E_0}\frac{1}{(\theta^2+\theta_E^2)}\operatorname{Im}\left(-\frac{1}{\epsilon(\Delta E)}\right), \quad (9)$$

where a_0 is the Bohr radius, θ is the angular deflection from the forward direction, $\theta_E=\Delta E/2E_0$, and $\epsilon(\Delta E)$ is the dielectric constant measured in an optical experiment.

If the boundary conditions at the surface of the crystal are taken into account as the electron approaches and then enters the crystal, there will be additional energy losses besides those described above. This problem was treated by Ritchie[10] on the basis of a hydrodynamical model and subsequently by Stern and Ferrel,[29] who added a factor which gives the angle-of-incidence dependence. These calculations yield the following expression for the differential probability that an electron loses energy ΔE and is scattered into $d\Omega$ while crossing one surface of the crystal:

$$\frac{d^2p}{d(\Delta E)d\Omega}=\frac{1}{2\pi^2 a_0 k_0 E_0}\frac{\theta}{(\theta^2+\theta_E^2)^2}\times f(\theta,\psi)\operatorname{Im}\left(\frac{(1-\epsilon)^2}{\epsilon(\epsilon+1)}\right), \quad (10)$$

where

$$f(\theta,\psi)=\left(\frac{1+\theta_E^2/\theta^2}{\cos^2\alpha}-(\tan\alpha\cos\psi+\theta_E/\theta)^2\right)^{1/2},$$

α is the angle of incidence, and ψ is measured relative to the plane of incidence.

Using the optical constants of silver measured by Ehrenreich and Philipp[30] and the attenuation coefficient estimates for low-energy electrons in silver made by Jones *et al.*,[25,31] the two contributions to $dP/d(\Delta E)$ defined in Eq. (7) can be calculated from Eqs. (9) and (10). The results of these calculations are shown in Figs. 13(a) and 13(b) for the appropriate experimental parameters given in the figures. The region between 3.5 and 3.8 eV in the surface-loss curves is drawn schematically to indicate a large narrow peak at $\operatorname{Re}(\epsilon)=-1$. The bulk term is much smaller than the

[29] E. A. Stern and R. A. Ferrel, Phys. Rev. **120**, 130 (1960).
[30] H. Ehrenreich and H. R. Philipp, Phys. Rev. **128**, 1622 (1962).
[31] Several other authors have obtained similar estimates of the attenuation coefficient for low-energy electrons in silver. See, for example, H. E. Farnsworth, Phys. Rev. **49**, 605 (1936); P. W. Palmberg and T. N. Rhodin, J. Appl. Phys. **39**, 2425 (1968).

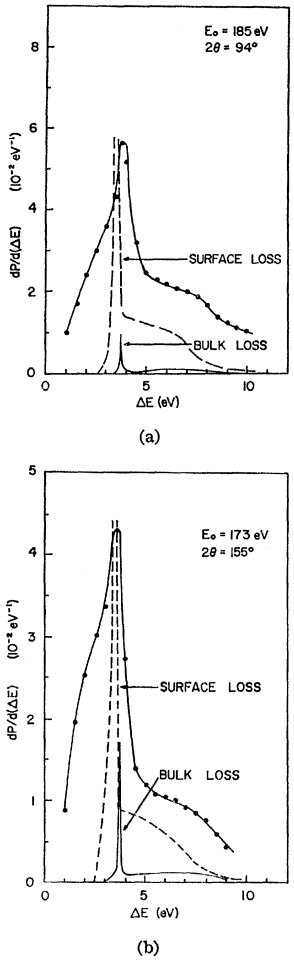

FIG. 13. Comparison between experimental and theoretical determinations of the quantity $dP/d(\Delta E)$ defined in Eq. (7). (a) $E_0=185$ eV and $2\theta=94°$. (b) $E_0=173$ eV and $2\theta=155°$.

surface term due to the factor

$$(e^{-2\mu d/\cos\alpha}/1-e^{-2\mu d/\cos\alpha})(d/\cos\alpha)$$

of Eq. (6). This factor gives the equivalent sample thickness for a transmission experiment and is 1.2 Å and 1.4 Å for the data in Figs. 13(a) and 13(b), respectively.

Experimental determinations of $dP/d(\Delta E)$ are also shown in Fig. 13. The theory predicts the structure in the energy-loss spectra quite well and gives the magnitude within a factor of two. The major discrepancy is that for $\Delta E<3$ eV the experimental energy-loss spectra are considerably larger than the theory predicts. This feature is also observed in the high-energy transmission data.[32]

The angular spreading measurements, which give a width of roughly $\Delta E/E_0$, are consistent with the θ dependence of either type loss. The experiments on the angle-of-incidence dependence, however, which show a larger inelastic-scattering probability at more grazing angles of incidence, indicate that the surface loss must be dominant. The surface-loss contribution to $dP/d(\Delta E)$ increases as α increases [through the factor $f(\theta,\psi)$ in Eq. (10)] and goes as $1/\cos\alpha$ for large α, while the bulk-loss contribution decreases as α increases, due to the attenuation.

In summary, we have shown quantitiativly that the inelastic intensity for $\Delta E<10$ eV in low-energy experiments arises from a two-step process involving both an elastic and an inelastic event. A simple model allows us to separate the Bragg and phonon contributions to the inelastic scattering and to obtain an energy-loss spectrum which is independent of the elastic scattering. The intensity, structure, angular widths, and the angle-of-incidence dependence of the experimental energy-loss spectra are compared to theory, giving reasonable agreement.

ACKNOWLEDGMENTS

The authors would like to thank R. L. Dennis for assistance in analyzing the data and Professor D. L. Huber for several helpful discussions regarding the interpretation of this work.

[32] See, for example, Figs. 35 and 45 of Ref. 19.